

1 **Supplementary Material**

2 **S1 Functioning of traits in JSBACH.**

3

4 **S1.1 SLA**

5 In JSBACH, SLA (specific leaf area (mol C m⁻²)) affects the size of the carbon pools. In the
6 default simulation SLA is a fixed PFT-specific parameter but in the variable traits simulation
7 it varies over time and is recalculated every year (based on local climatic conditions, see
8 Table 2 in main text). In all other aspects, SLA functions in the same ways as in the default
9 model (see below).

10 The NPP determines vegetation carbon pools. NPP is allocated using fixed
11 proportions into green (living, both above and below ground), wood (both above and below
12 ground) and reserve pools, as well as root exudates. Limits are set to the different pools; the
13 wood pool has a PFT-specific maximum carbon content. For the green pool, SLA determines
14 in combination with LAI (-) and a pool-specific ratio of pool carbon to leaf carbon (c_g, 4.0 (-)
15 for all PFTs) the maximum amount of carbon that can be stored in the green pool (C_G^{max}):

16

17
$$C_G^{max}(t) = \frac{c_g}{SLA} LAI(t) \quad (1)$$

18

19 For the reserve pool not the maximum but an optimal amount of carbon content (C_R^{opt}) is set
20 by the same formula (only with a different ratio-parameter, (c_r, with a value of 2.0 (-) for
21 forests and shrubs and 4.0 (-) for grasses), as this pool is not emptied when LAI decreases.
22 Consequently the reserve pool can be larger than the optimal value:

23

24
$$C_R^{opt}(t) = \frac{c_r}{SLA} LAI(t). \quad (2)$$

25

26 *Reference:*

27 Parida, B.R.: The influence of plant nitrogen availability on the global carbon cycle and N₂O
28 emissions, MPI-M report on the Earth System Science, nr. 92, 141 pp, 2011.
29 (http://www.mpimet.mpg.de/fileadmin/publikationen/Reports/WEB_BzE_92.pdf)

30

31 **S1.2 Vcmax₂₅ and Jmax₂₅**

32 Vcmax₂₅ and Jmax₂₅ (maximum carboxylation and electron transport rate at a reference
33 temperature of 25 °C (μmol m⁻² s⁻¹), respectively) are used to calculate Vcmax and Jmax
34 values at actual temperatures. In the default simulation Vcmax₂₅ and Jmax₂₅ are PFT-specific
35 fixed values but in the variable traits simulation they vary over time. They are recalculated
36 every year (based on local climatic conditions, see Table 2 in main text). Afterwards, the
37 same photosynthesis routine as the default mode is followed (see equations below taken after
38 Knorr (1997)).

39

40 *C3 plants*

41 For C3 plants, the temperature dependence of Vcmax and Jmax is calculated following
42 Farquhar (1988):

43

$$44 Vcmax = Vcmax_{25} f(T) \exp\left(\left(\frac{T}{T_{ref}} - 1\right) \frac{E_V}{RT}\right) \quad (3)$$

45

$$46 Jmax = Jmax_{25} f(T) \exp\left(\left(\frac{T-T_0}{T_{ref}-T_0}\right)\right) \quad (4)$$

47

48 T is the temperature in °K, E_V is the activation energy (58520 J mol⁻¹) and R is the gas
49 constant (8.314 J mol⁻¹ K⁻¹). T_{ref} (298.15 K) and T_0 (273.15 K) are reference temperatures. In
50 either formula, V_{cmax25} and J_{max25} are fixed in the default simulation but vary in the
51 variable traits simulation. For both V_{cmax} and J_{max} , an additional formula accounting for
52 high temperature inhibition ($f(T)$) is included (Collatz et al. 1991):

53

54
$$f(T) = \frac{1}{(1+e^{1.3(T-T_1)})}, \quad (5)$$

55

56 with T_1 as reference temperature (328 K).

57 Actual V_{cmax} is then used to calculate carboxylation rate (J_C) (Farquhar et al.
58 (1980)):

59

60
$$J_C = V_{cmax} \frac{c_i - \Gamma_*}{c_i + K_C(1+O_i/K_O)} \quad (6)$$

61

62 Here c_i and O_i are the CO₂ and O₂ concentrations inside the leaf (μmol (CO₂) mol⁻¹ (air) and
63 mol (O₂) mol⁻¹ (air), respectively), Γ_* is the CO₂ compensation point (μmol (CO₂) mol⁻¹ (air))
64 and K_C and K_O are the Michaelis-Menten constants for CO₂ and O₂ (μmol (CO₂) mol⁻¹ (air)
65 and mol (O₂) mol⁻¹ (air), respectively). K_C , K_O and Γ_* are temperature dependent, see
66 Farquhar (1988) for equations.

67 With actual J_{max} electron transport rate (J_E) is calculated (Farquhar et al. (1980)):

68

69
$$J_E = J(I) \frac{c_i - \Gamma_*}{4(c_i + 2\Gamma_*)}, \quad (7)$$

70

71 with the function $J(I)$:

72

73
$$J(I) = J_{max} \frac{\alpha I}{\sqrt{J_{max}^2 + \alpha^2 I^2}}, \quad (8)$$

74

75 where $I = I_{PAR} / E_{PAR}$. I_{PAR} is the PAR absorption rate ($W m^{-2}$) and E_{PAR} is the energy content
 76 of PAR (220 kJ mol^{-1} (photons)) and α (0.28, (-)) is the quantum efficiency for photon
 77 capture.

78 Net carbon assimilation (A) is the minimum of Eq. (6) and Eq. (7) minus dark
 79 respiration:

80

81
$$A = \min(J_C, J_E) - R_d \quad (9)$$

82

83 Dark respiration at a references temperature of 25°C ($R_{d,25}$) is a fixed fraction of
 84 $Vcmax_{25}$, meaning that in contrast to a fixed values in the default simulation, $R_{d,25}$ varies as
 85 well in the variable traits simulation:

86

87
$$R_{d,25} = \gamma Vcmax_{25}, \quad (10)$$

88

89 with γ (-) having a value of 0.011 (Farquhar 1980). Actual R_d is calculated following Von
 90 Caemmerer (2000)):

91

92
$$R_d = R_{d,25} f(T) g(Ir) \exp\left(\left(\frac{T}{T_{ref}} - 1\right) \frac{E_R}{RT}\right), \quad (11)$$

93

94 where E_R is the activation energy (45000 J mol^{-1}). Irradiance inhibition ($g(Ir)$) is calculated as
 95 follows:

96

97
$$g(Ir) = 0.5 (1 + e^{-Ir/10}), \quad (12)$$

98

99 with Ir being total irradiance at the surface (mol (photons) m⁻² s⁻¹).

100

101 *C4 plants*102 C4 plants follow a similar routine as C3 plants; only the equations for carboxylation and
103 electron transport rate differ (Collatz et al (1992)). Carboxylation rate is calculated using
104 PEPcase CO₂-specificity (k (mol m⁻² s⁻¹)) instead of Jmax:

105

106
$$J_C = k c_i, \quad (13)$$

107

108 with k being calculated from a reference k at 25 °C (k₂₅):

109

110
$$k = k_{25} \exp\left(\left(\frac{T}{T_{ref}} - 1\right) \frac{E_K}{RT}\right) \quad (14)$$

111

112 As with Jmax₂₅ for other PFTs, k₂₅ is fixed in the default simulation and recalculated every
113 year in the variable traits simulation before being input in the above formula. E_K is the
114 activation energy (50967 J mol⁻¹).

115 Electron transport rate is calculated as follows:

116

117
$$J_E = \frac{1}{2\theta_s} (Vcmax + J_i - \sqrt{(Vcmax + J_i)^2 - 4\theta_s Vcmax J_i}) \quad (15)$$

118

119 V_{cmax} is calculated from $V_{cmax_{25}}$ in the same way as C3 plants, and θ is the curve
120 parameter for J_E (0.83 (-)), and J_i calculated as:

121

122 $J_i = \alpha_i I,$ (16)

123

124 where α_i is the integrated C4 quantum efficiency (0.04 mol (C) $m^{-2} s^{-1}$). As for C3 plants,
125 $R_{d,25}$ is also proportional to $V_{cmax_{25}}$ (Eq. (10)), but with a γ of 0.042.

126

127 *References:*

128 Collatz, G.J., Ball, J.T., Grivet, C. and Berry, J.A.: Physiological and environmental
129 regulation of stomatal conductance, photosynthesis and transpiration: a model that includes a
130 laminar boundary layer, *Agr. Forest Meteorol.*, 54, 107-136, doi: 10.1016/0168-
131 1923(91)90002-8 1991.

132 Collatz, G. J., Ribas-Carbo, M., and Berry, J. A.: Coupled photosynthesis-stomatal
133 conductance model for leaves of C₄ plants, *Aust. J. Plant Physiol.*, 19, 519-538, 1992.

134 Farquhar, G.D.: Models relating subcellular effects of temperature to whole plant
135 responses, in: *Plants and Temperature*, Long,S.P. and Woodward, F.I. (Eds), 1988, Biologists
136 Limited, Cambridge, U.K., 395-409, 1988.

137 Farquhar, G. D., Caemmerer, S. V., and Berry, J. A.: A biochemical model of
138 photosynthetic CO₂ assimilation in leaves of C₃, *Planta*, 149, 78-90,
139 doi: 10.1007/BF00386231, 1980.

140 Knorr, W.: Satellite remote sensing and modelling of the global CO₂ exchange of land
141 vegetation: a synthesis study, Ph.D. thesis, University of Hamburg, Germany, 189 pp., 1997.

142 Knorr, W., and Heimann, M.: Uncertainties in global terrestrial biosphere modeling 1.
143 A comprehensive sensitivity analysis with a new photosynthesis and energy balance scheme,
144 Global Biogeochem. Cy., 15, 207-225, doi: 10.1029/1998gb001059, 2001.

145 Von Caemmerer, S.: Biochemical models of leaf photosynthesis, CSIRO Publishing,
146 Collingwood, Australia, pp. 165 pp. 2000.

147

148

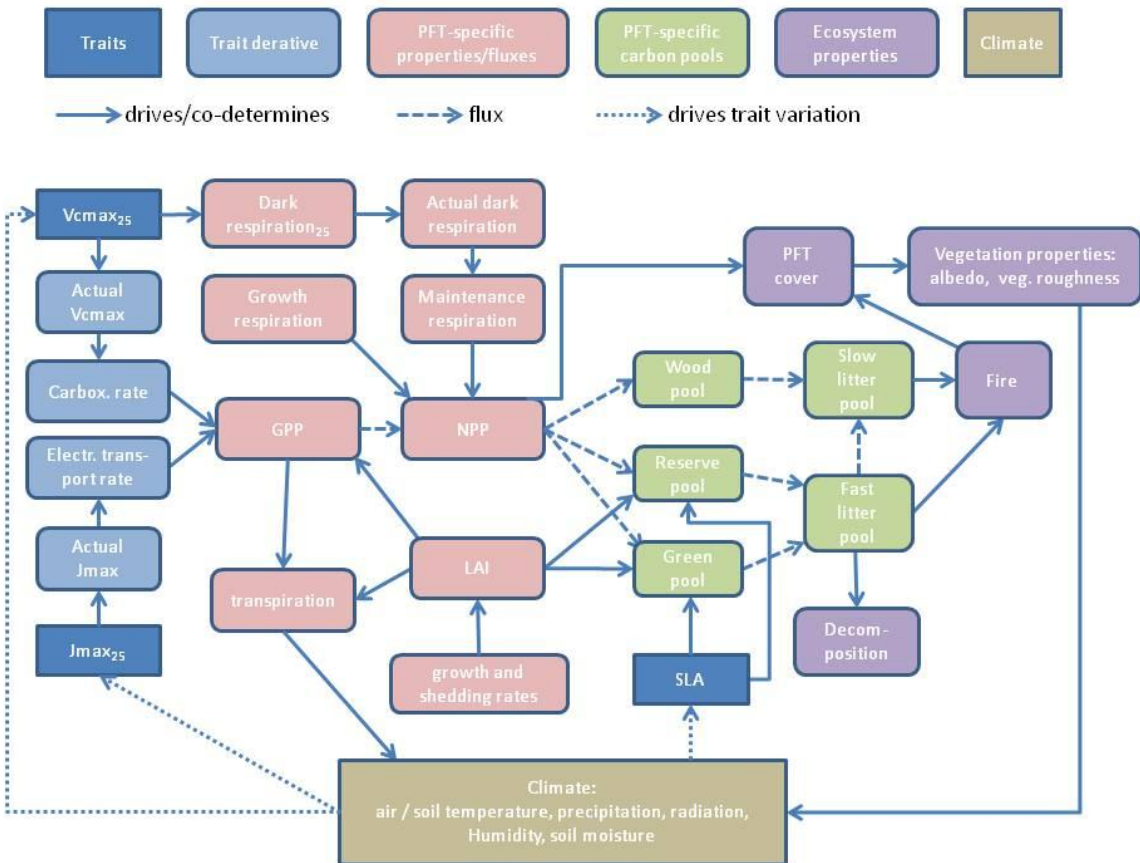
149 **S2 Role of the selected traits in JSBACH processes.**

150 Fig. S2.1 shows a flowchart with the different roles of the selected traits in JSBACH
151 processes. It demonstrates how variation in traits might propagate in JSBACH and affect
152 PFTs, ecosystem properties and climate.

153 Actual V_{cmax} and J_{max} are used to model carboxylation and electron transport rate,
154 which, combined with dark respiration, determine GPP (see S1.2). GPP minus growth and
155 maintenance respiration (scaled to canopy from dark respiration) determines NPP.
156 Productivity in turn affects transpiration, which will modify soil moisture and air
157 temperature. Effects of variation in V_{cmax25} and J_{max25} propagate via NPP, which
158 determines the competitive ability of PFTs and consequently PFT cover and ecosystem
159 properties. Differences in fractional coverage of PFTs result in differences in vegetation
160 properties like albedo and vegetation roughness, modifying heat and water fluxes, which
161 affect temperature and precipitation. SLA (see S1.1 for calculation of SLA) effects on climate
162 are more moderate, but it co-determines carbon storage in the green and reserve pool and as
163 such affects the amount of litter going to the litter pools, indirectly influencing decomposition
164 rates and fire frequency as well.

165 In turn, climatic conditions are used to predict trait values on a yearly basis (dotted
166 lines). Climate also directly drivers many other processes (e.g. actual V_{cmax} and J_{max} ,
167 transpiration, leaf and shedding rates, fire frequency etc.) but these have been omitted for
168 clarity.

169



170

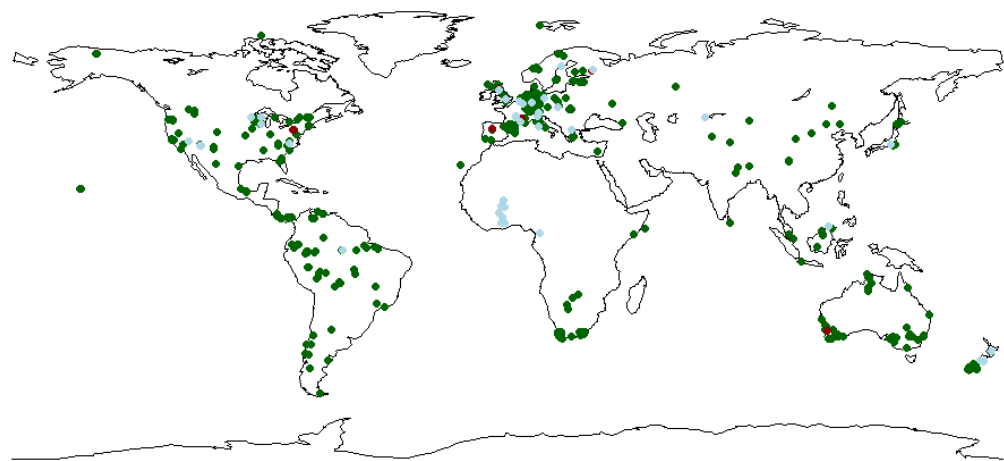
171 Fig. S2.1. Flowchart with the functioning of SLA, V_{cmax25} and J_{max25} in JSBACH and their
172 effects on PFTs, ecosystem properties and climate.

173

174

175

176 **S3 World map with locations from which trait data were used in this study.**



177

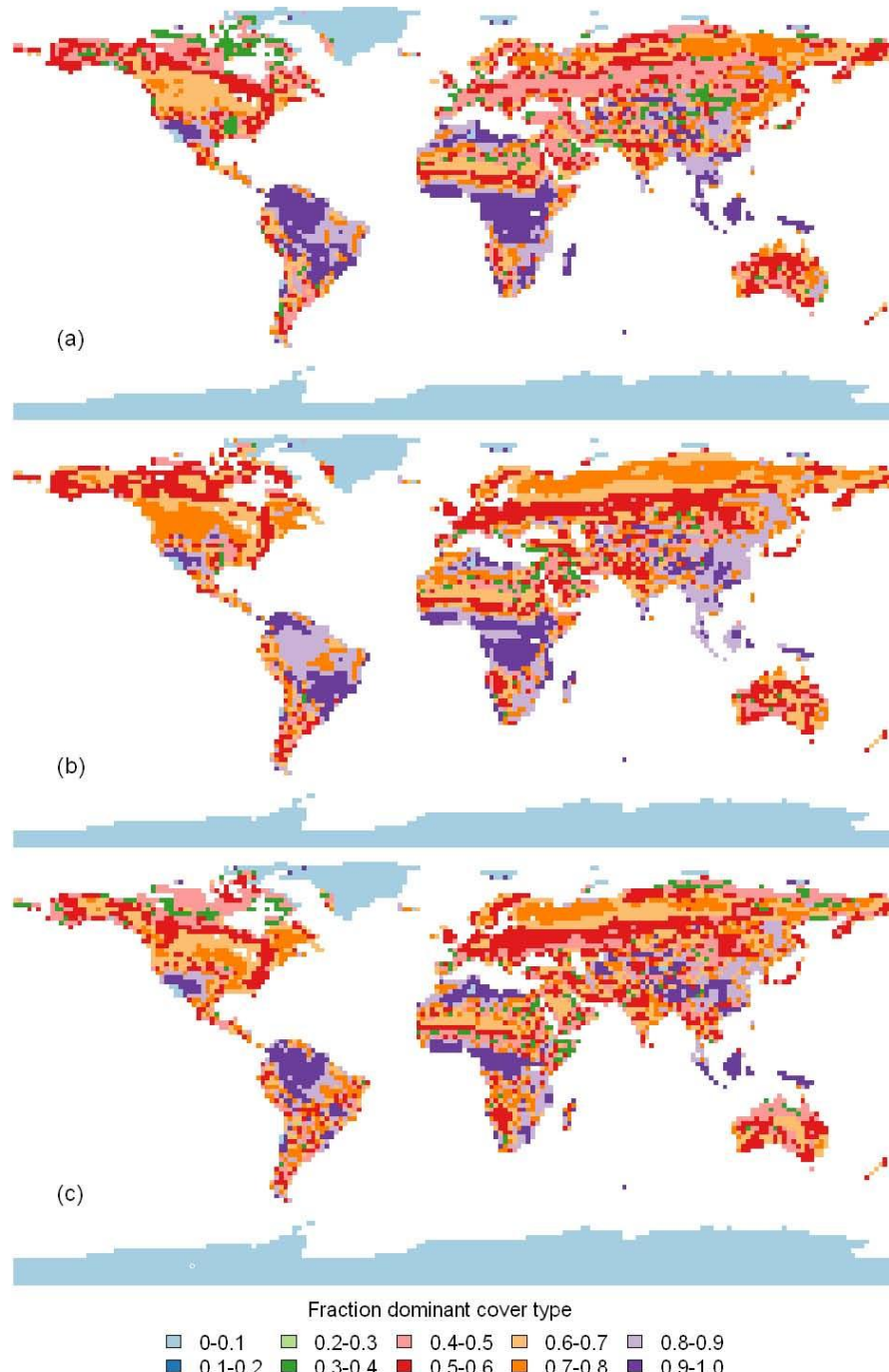
178 Fig S3. Locations with trait data used in this study. Green dots SLA, red dots V_{cmax25} only,
179 and blue dots indicate locations with both V_{cmax25} and J_{max25} data.

180

181
182

183

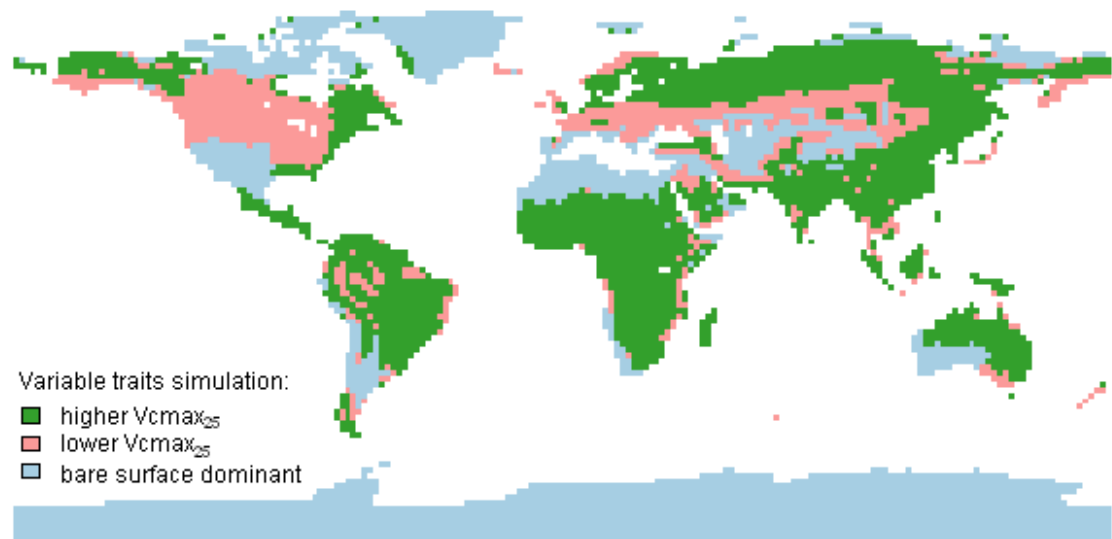
184 S4 World map of fractional coverage of dominant cover type (including
185 bare soil).



186
187 Fig. S4.1. Fractional coverage of dominant cover type (including bare soil). (a) default
188 simulation, (b) observed traits simulation and (c) variable traits simulation.

189 **S5 World map showing V_{cmax25} of the dominant PFTs in the variable
190 traits simulation relative to the default simulation.**

191



192
193 Fig.S5.1. V_{cmax25} of the dominant PFTs in the variable traits simulation relative to the
194 default simulation. The dominant PFTs in the variable traits simulations have higher V_{cmax25}
195 than the default simulation in the green areas and lower V_{cmax25} in the pink areas. In blue
196 areas bare ground (or ice) is the dominant cover type.

197

198

199

200 **S6 Comparisons between predicted dominant vegetation maps of the three**
201 **simulations with the potential vegetation map of Ramankutty and Foley**
202 **(1999).**

203

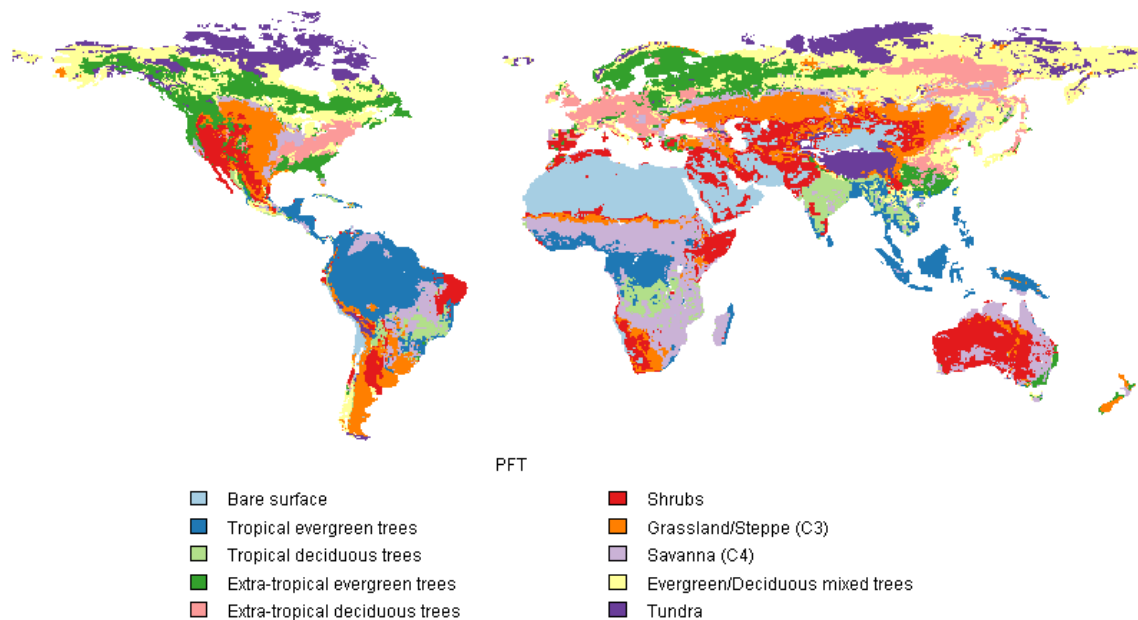
204 Table S6.1. Aggregation of PFTs in Ramankutty and Foley to match JSBACH PFTs.

JSBACH	PFT
bare	desert
tropical broadleaved evergreen trees	tropical evergreen forest/woodland
tropical broadleaved deciduous trees	tropical deciduous forest/woodland
extra-tropical evergreen trees	temperate broadleaf evergreen forest/woodland temperate needleleaf evergreen forest/woodland boreal evergreen forest/woodland
extra-tropical deciduous trees	temperate deciduous forest/woodland boreal deciduous forest/woodland
shrubs (raingreen and deciduous)	dense shrubland open shrubland
C3-grasses	grassland/steppe
C4-grasses	savanna
--	tundra
--	evergreen/deciduous mixed forest/woodland

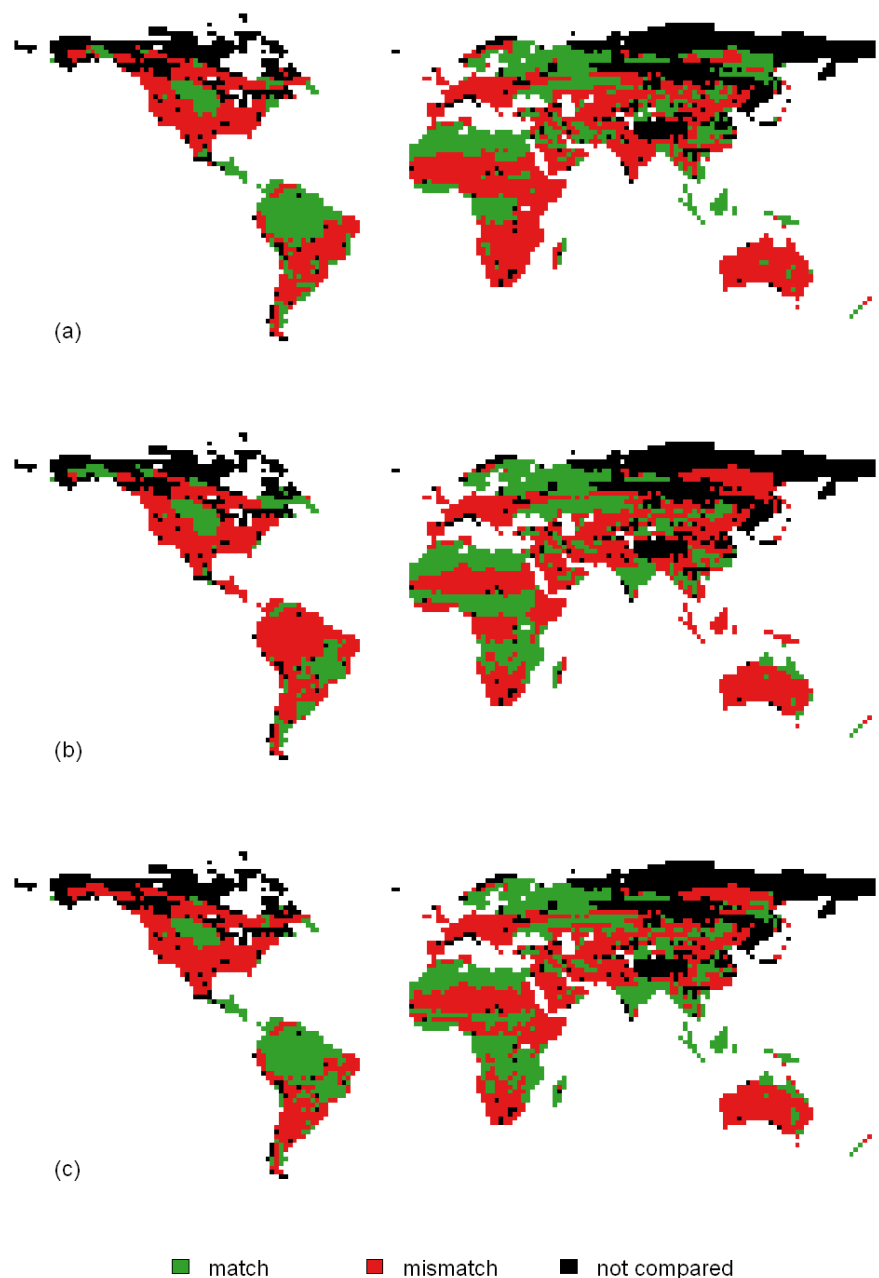
205

206

207



210 Fig. S6.1. Potential vegetation map with aggregated PFTs (see table S6.1).
 211 Evergreen/deciduous mixed forest and tundra were omitted from the comparisons with
 212 JSBACH vegetation distribution.



214

215 Fig. S6.2. (Mis-)match between simulations and aggregated potential vegetation map for (a)
 216 default simulation, (b) observed traits simulation and (c) variable traits simulation.

217

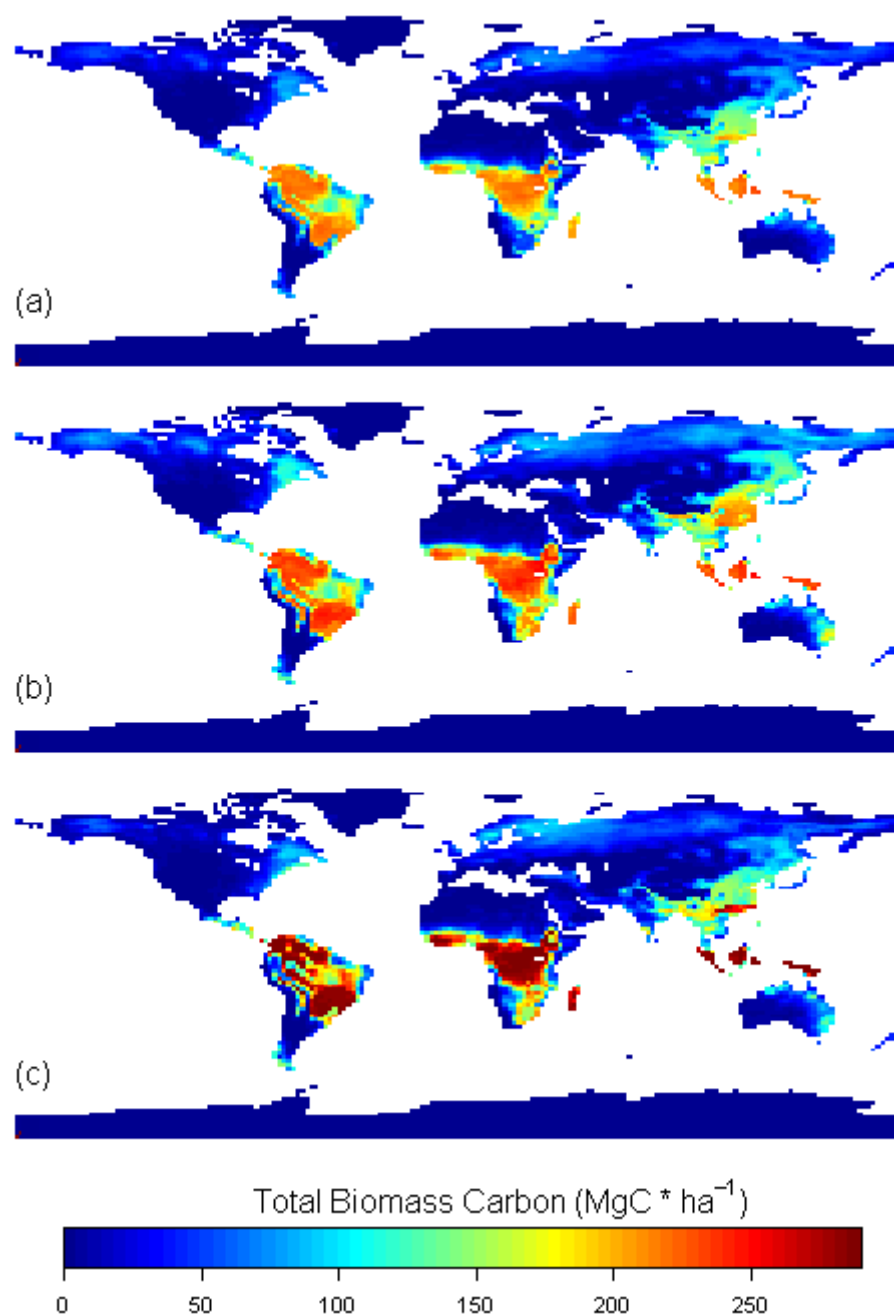
218

219

220

221 **S7 World map with simulated total biomass carbon in vegetation.**

222



223

224 Fig. S7.1. Total biomass carbon (MgC ha^{-1}) of (a) default simulation, (b) observed traits
225 simulation and (c) variable traits simulation.

226